International Journal of Engineering & Technology, 7 (3.34) (2018) 122-128

International Journal of Engineering & Technology

Website: www.sciencepubco.com/index.php/IJET

Research paper

Propagation Characteristics of Debris Flows Considering Entrainment Effect

Seokil Jeong[1], Junseon Lee[2], Chang Geun Song[3], Seung Oh Lee[1*]

[1]*Department of Civil Engineering, Hongik University, 94, Wausan-ro, Seoul, 04066, Korea.*
[2]*Department of Civil Engineering, West Virginia University, Morgantown, 26506, USA*
[3]*Department of Safety Engineering, Incheon National University, 119, Academy-ro, Incheon, 09571, Korea.*
**Corresponding author E-mail: seungoh.lee@hongik.ac.kr*

Abstract

Background/Objectives: Due to the extreme climate and the localized heavy rain, the frequency of debris flow has been increasing. Therefore, there is a growing expectation for accurate numerical analysis.
Methods/Statistical analysis: We present a prediction method that can calculate the propagation length of the debris flow. This analysis indicates the relationship between the potential energy and the propagation length of the debris flow. To study the behavior of the debris flow accurately, the change in the momentum force must be considered; otherwise the calculation accuracy of the debris flow behavior is inevitably low.
Findings: Entrainment is a common behavior in a debris flow that leads to changes in the momentum force. Here, we analyzed the change in the momentum force using a 2D simulation model that included entrainment. The results show how the debris flow behaves with changes in the momentum force. When entrainment is considered, the propagation length tends to be underestimated. With detailed information, the uncertainty in the prediction accuracy can be reduced.
Improvements/Applications: If studies on the material properties of debris flow would be added, it will be possible to carry out various and accurate analysis of the debris flow

Keywords: *Debris flow, Entrainment, Numerical simulation, Froude number, Propagation length*

1. Introduction

The behavior of a debris flow is complex and many factors must be considered to predict its flow. These issues can be resolved by precise simulation; however, this costs a lot of time and requires highly accurate input data for successful analysis. Various studies have been conducted to solve this complexity. Most of them have generally been based on the observed debris flow. For instance, the debris flow using observed values from the Swiss Alps area was analyzed [1]. The observed data showed that the debris flow propagated further in unobstructed and V-shaped terrain. On the other hand, when the amount of debris flow was less than $10^4 \mathrm{m}^3$ in mountainous terrain, the flow propagated over a relatively short distance. The following equation was derived from this feature of the debris flow.

$$L = 1.9V^{0.16}H^{0.83} \quad (1)$$

where L is propagation distance, H is the height where the debris flow occurred, and V is the amount of debris flow (correlation coefficient r^2=0.75). It was studied about the behavior of the debris flow based on the height and the amount where the debris flow occurred. The results were, therefore, based on a topographical point of view [1]. A mechanism of the debris flow using the ratio of the drop height and the runout distance of the debris flow was presented in Figure 1 [2].Other studies analyzed the behavior of the debris flow using analytical solutions, which can be calculated using the momentum as follows.

$$s_T = A_V^2/\mathrm{G}$$

$$A_V = v_u \cos(\theta_u - \theta)\,[1 + \mathrm{g}\square_u \cos\theta_u/(2v_u^2)] \quad (2)$$

where $s_T$is runout length,θ is the slope of the bottom angle, θ_u is the entry channel slope angle, v_u is entry velocity, $\square_u$ is entry flow depth, and S_f is friction slope [3, 4].

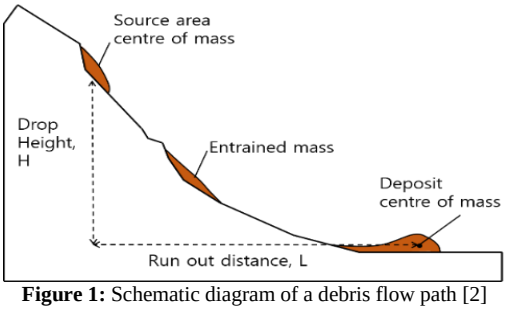

Figure 1: Schematic diagram of a debris flow path [2]

Recent studies have provided a simple analysis of the behavior of a debris flow; however, these studies lack accuracy and applicability. This disadvantage is resulted from the exclusion of the change in momentum force, which is a significant element in a debris flow. Thus, some researches have been focused the entrainment phenomenon to consider such momentum force. The entrainment equation of a debris flow was compared the

calculated values with experimental results [5]. The erosion and deposition of a debris flow was described [6]. A definition for the entrainment phenomenon of a debris flow, and guidelines for the prediction of debris flows was suggested [7]. The mechanisms and equations for the entrainment of a debris flow were provided by a series of experiments [8]. The bed erosion initiated by a dam collapse was simulated [9]. And, laboratory model experiments and numerical simulations to describe the entrainment of a debris flow were performed [10]. Various observations on actual debris flows were compiled and numerical simulations using the particle analysis of debris flows were conducted [11].Previous studies based on the momentum force have, however, experienced several problems in terms of cost and consistency because they mainly focused on observed data of debris flows. The aim of this study was to resolve these problems using a numerical approach by analyzing the change in the momentum force.

2. Simulation Model

2.1. Computational Models

A 2D rheological model was used to simulate the behavior of a debris flow [12]. The equation includes the effective turbulent stress, pressure, shear stress, and gravity acting on the debris flow. The mathematical models for predicting the movement of the debris flow are shallow water equations, which are classified into two categories: conservative and non-conservative types. In this study, the non-conservation shallow water equations as presented in Eq. (3) were chosen because they are suitable for describing rapid flows on steep terrain.

$$\frac{\partial h}{\partial t} + h\frac{\partial u_j}{\partial x_j} + u_j\frac{\partial h}{\partial x_j} = -\frac{\partial b}{\partial t} \tag{3-1}$$

$$\frac{\partial u_i}{\partial t} + u_j\frac{\partial u_i}{x_j} = -g\frac{\partial H}{\partial x_i} - g\frac{\partial \square}{\partial x_i} + \frac{\partial}{\partial x_i}\left(\nu\frac{\partial u_i}{\partial x_i}\right) - \frac{\tau_b}{\rho_D \square} \tag{3-2}$$

where h is water depth, t is time, x and y are the longitudinal and transverse directions in Cartesian coordinates, respectively, H is elevation of the channel bottom, ρ is the bulk density of the debris flow, ν is kinematic viscosity, and τ_b is bottom shear stress. In describing the run-out of debris flow, bottom shear stress is an important factor because it activates the resistance and the stop-and-go mechanism. Bingham and Vollemy models have been used extensively in simulations [13]. In this study, the Coulomb equation was applied because it gave satisfactory results with one adjustable parameter, the internal friction angle.

$$\tau_b = \rho g h \cos\theta \tan\theta_b \tag{4}$$

where θ is the slope of the bottom angle, and θ_b isthe angle of internal friction, which is defined as the angle between soils. It is 0° in clay and 30°–40° in sand, and less than 10° in a normal debris flow.

To discretize the governing Eq. (3), the SU/PG scheme, which is a Petrov-Galerkin stabilizing method, was used because it provides stable solutions under abrupt flow change, such as, dam collapse, flood flow, or transitional flow [14].

2.2. Entrainment Term

There are various expressions of entrainment. The physical meaning of entrainment of a debris flow is the bed erosion caused by the density difference between the bed material and the debris flow. Therefore, the thickness and amount of erosion should be estimated to account for entrainment. The calculation with this method was suggested [15].

$$\rho\square\frac{\partial v_x}{\partial t} = \rho\square g_x + k_x\sigma_z\left(-\frac{\partial\square}{\partial x}\right) + k_{xy}\sigma_z\left(-\frac{\partial\square}{\partial y}\right) + \tau_{zx} - \rho v_x\frac{\partial b}{\partial t} \tag{5}$$

$$\rho\square\frac{\partial v_y}{\partial t} = \rho\square g_y + k_y\sigma_z\left(-\frac{\partial\square}{\partial y}\right) + k_{xy}\sigma_z\left(-\frac{\partial\square}{\partial x}\right) + \tau_{zy} - \rho v_y\frac{\partial b}{\partial t}$$

where x and y are the longitudinal and transverse directions in Cartesian coordinates, respectively, ρ is the bulk density of the debris flow, h is the debris flow depth, v is debris flow velocity, g is the acceleration due to gravity, τ is the shear stress, b is the bed-normal erosion depth, k_x, k_{yx}, k_y, and k_{xy} are stress coefficients that normalize the tangential normal and shear stresses near the bed with respect to the total bed-normal stress, and σ_z is total bed-normal stress:

$$\sigma_z = \rho h(g\cos\theta + a_z) \tag{6}$$

where θ is the slope of the bottom angle, and a_z is the centripetal acceleration due to the curvature of the path in the direction of motion.Bed erosion with respect to time is defined as the erosion rate$\left(\frac{\partial b}{\partial t}\right)$. The erosion rate represents the discharge of material entering a debris flow. The factors related to the erosion rate are bottom slope, density, and flow velocity. Considering these, a simplified equation for erosion rate can be obtained as follows [5].

$$\frac{\partial b}{\partial t} = \alpha v\frac{C_e - C}{C_* - C_e}\frac{\square}{d}\left(\frac{\partial b}{\partial t} \geq 0\right) \tag{7-1}$$

$$\frac{\partial b}{\partial t} = \beta v\frac{C_e - C}{C_* - C_e}\frac{\square}{d}\left(\frac{\partial b}{\partial t} < 0\right) \tag{7-2}$$

where α and $\beta$are experimental coefficients, $C_e$is the equilibrium sediment concentration of the debris flow by volume corresponding to the bed slope,θ; $C_*$is the sediment concentration by volume of bed sediment (non-moving layer), $C$is the sediment concentration of debris flow by volume corresponding to bed slope,θ; $h$is debris flow depth, and $d$is the grain size of the debris flow.As shown in Eq. (7) [5] is based on an equilibrium slope including erosion and sedimentation. The erosion rate using the total amount of debris flow, the total amount of erosion, and the average transport length were applied to Eq. (7) and were simplified as shown in Eq. (8) [16].

$$\frac{\partial b}{\partial t} = \bar{E}hv \tag{8}$$

where h is the thickness of debris flow, v is flow velocity, and $\bar{E}$ is the average growth rate defined by

$$\bar{E} = \frac{\ln(V_f/V_0)}{\bar{S}} \tag{9}$$

where V_0 is the estimated initial amount of debris flow entering, V_f is the estimated totalamount of debris flow, and $\bar{S}$ is the approximate average path length.This erosion rate is closely related with the growth rate. It is assumed that the growth rate is independent of the velocity of the debris flow. If $\bar{E}$ is 0.01 m^{-1}, the discharge of debris flow increases to 1% per meter. This type of entrainment equation has the benefit that it simplifies complicated phenomena. Accordingly, $\bar{E}$ implicitly includes comprehensive parameters such as the velocity of the debris flow, the slope angle, the curvature path, the surface roughness, and the characteristics of the bottom surface.

3. Model Verification

3.1. Field-Scale Experiment

There is a lack of data on the actual debris flow events, and it is difficult to test the feasibility of model application. In this case, it is usual to adopt appropriate approaches such as performing hydraulic experiments or referring to previous studies. In this study, to verify the model performance, the field-scale

experiments carried out by USGS were considered as presented in Figure 2.Longitudinal distance is measured from the gate at the head of the channel, and debris-flow front position as a function of time since flow release during eight entrainment experiments. The experiments recorded the thickness, velocity, and impact force of the debris flow. The results of various experiments compiled [17] were taken as a reference for the verification simulations. Unknown properties, such as the Coulomb angle, were obtained by the comparison with experimental results.

By analyzing the simulation results, we could determine the appropriate range of simulation conditions (see Table 1). The range of this property value was selected as the case that can most closely reflect the results of the USGS experiment. As shown in Table 2, the propagation length and the velocity of the debris flow could be simulated within an error of approximately 6–25%. Based on this analysis, the Coulomb angle was set as 3°, which is one of the commonly observed Coulomb values for debris flows.

Table 1: Experimental results from USGS [17]

USGS Experimental results	Velocity range	Propagation Length
	6.5–10.5 m/s	25–30 m

Table 2: Numerical results for calibration

Coulomb angle (θ)	Length (m)	Velocity (m/s)	Average error (%)
1°	31.97	9.06	22.88
2°	28.95	8.73	7.94
3°	25.93	8.42	6.70
4°	24.92	7,94	15.92
5°	23.91	7.60	23.61

With the optimized simulation conditions, numerical results of front location of debris flow were compared with the values reported in previous literatures [18, 19, 20]. This experiment showed that the bed erosion was 0.1 cm at the flow channel section of 6–53 m. Using the entrainment equation [16], the growth rate was calculated as 0.02 m^{-1}. With this value, other numerical simulations were performed, and the velocity of the debris flow (8 m/s) was almost the same as that of the USGS experiment and the results of the simulation. This shows that the numerical model used in this study appropriately simulated the behavior of the debris flow with entrainment as shown in Figure 2 (b).

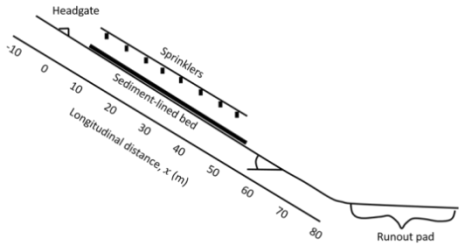

(**a**)

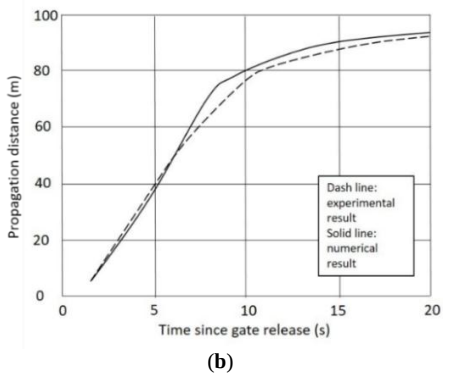

(**b**)

Figure 2: Entrainment experiment; (a) schematic cross-section of the flume experiment configuration showing the upper headgate area; (b) comparison with numerical and experimental results.

3.2. Field Runout Event

To verify the entrainment equation presented above, comparisons with observed debris flow were done. The DAN model was applied to the actual field event occurred in British Columbia, Canada [16]. They determined a growth rate of $\bar{E} = 1.9 \times 10^{-3} m^{-1}$ by using Eq. (9) with $V_f = 735{,}000\ m^3$, $V_0 = 375{,}000\ m^3$, and $S = 350$ m based on measured data. The numerical model developed in this study was run using this value. The simulation result showed an error range of about 20 m compared with the actual debris flow. A comparison of the observed debris flow and the simulated results showed that the entrainment equation properly reflected the behavior of the actual debris flow as shown in Figure 3.

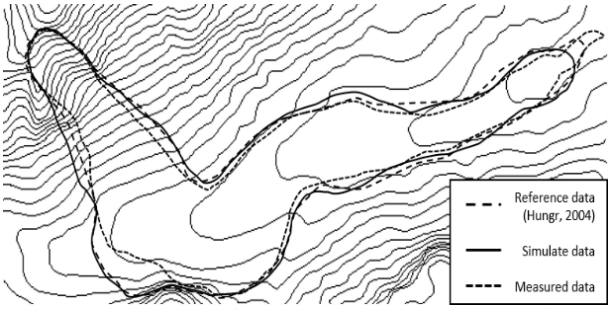

Figure 3: Comparison of the simulated and measured debris flows

4. Parameter Determination for Debris Propagation

The physical property data for the numerical simulations were input using previous verification. The terrain information was set up to be able to reflect the actual flow characteristics. The range of the growth rate, which is the most important factor in this study, was estimated from several simulation results. As a result, the characteristic of entrainment was underestimated in the case of $\bar{E} < 0.01\ m^{-1}$, whereas it was overestimated with $\bar{E} > 0.05\ m^{-1}$. The criterion of growth rate was set based on these characteristics.

4.1. Physical Properties

The physical properties data such as density, eddy viscosity, and the Coulomb angle are necessary to execute the numerical model. Using the verification results and references, the property values were set as presented in Table 3.

Table 3: Physical properties

Input	Value
Density	1,835 kg/m^3
Eddy viscosity	8 m^2/s
Coulomb angle	3°

4.2. Boundary Conditions and Topography

The conditions for inflow and outflow boundary were prescribed as flux-in and flux-out, respectively as shown in Table 4. The side boundaries had slip conditions. The size of the finite element was 10 m. The initial debris flow volume was set as 4,000 m^3 with reference to the actual initial debris flow volume. The simulation was continued until its initial mass passed the domain out, which corresponds to 50 s. The time step was 0.01 s so that the motion of the debris flow could be accurately captured. The conditions of entrainment were represented by a growth rate of $\bar{E} = 0.1$–$0.5 m^{-1}$.

Table 4: Input conditions for numerical simulations

Input condition	Value
Inflow boundary	Flux in

Outflow boundary	Flux out
Wall boundary	slip
Initial debris flow volume	$20 \times 40 \times 5$ m^3
Total time	50 s
Time interval	0.01 s
Roughness coefficient	0.05
Dry depth	0.002 m
Growth rate	0.0033, 0.0066, 0.01, 0.0133, 0.0166, 0.02, 0.0233, 0.0266, 0.03 m^{-1}

The actual debris flow occurred in unspecified topographical shapes. However, the majority of the debris flow was initiated in valleys or canyons. To reflect these characteristics, the topography was produced as V-shape, which shows that the behavior of the debris flow was concentrated in one direction (see Figure 4). The slope of the sliding side was set as 30°, which is the slope of the most common debris flow. The slope of the propagation surface with the actual debris flow was estimated to be less than 5°. This slope is considered the maximum slope of the propagating surface. Based on these characteristics, the propagating surface of the slope was set to 0°. The simulation could, therefore, be run with less error because the simulation value converged rapidly. The onset of debris flow was assumed to follow the dam collapse instance. Although debris flows can be initiated from various initial shapes, hexahedral mass break was considered. The topography used in this simulation was representative of the terrain where the debris flow occurred.

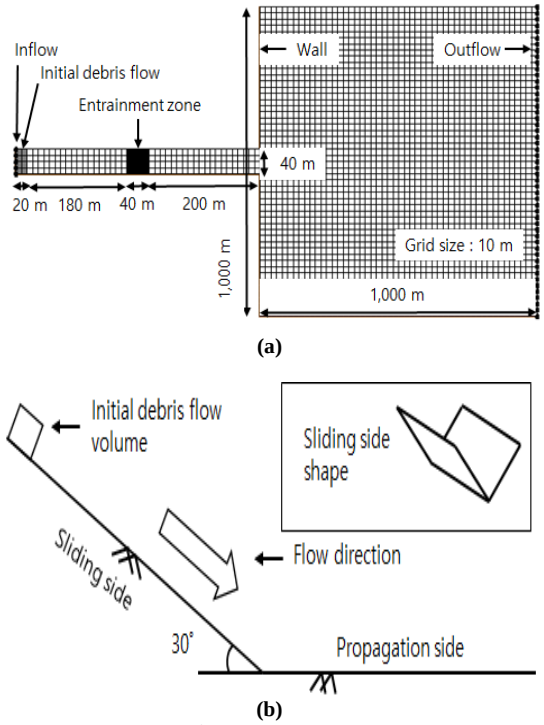

Figure 4: The topography of the simulation: (a) boundary conditions and the size of the topography, (b) side view of topography

5. Propagation of Debris Flow Considering Entrainment

The propagation length of the debris flow indicates the position of the end of the flow. According to Figure 5, the influence of entrainment became notable after 15 seconds of its occurrence. In other words, after the debris flow moved 240 meters downstream, the effect of entrainment predominantly activated [22].As the growth rate increased, the propagation length also increases at a constant rate. Similar to previous studies, the propagation length tended to increase when the amount of debris flow was larger, and the maximum propagation length bounded between 430 m and 650 m.

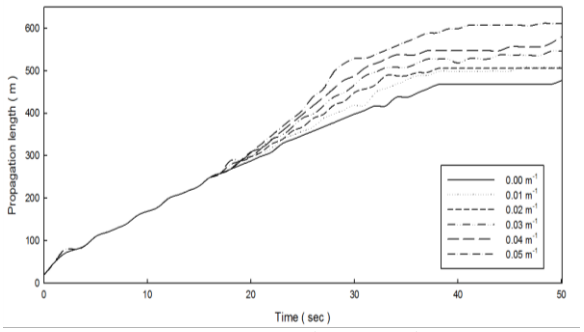

Figure 5: Propagation length of the debris flow with time

Figure 6 shows that entrainment clearly affected the propagation length of the debris flow. To clarify the influence of entrainment, we varied the amount of debris flow and growth rate as following as Eq.(9). First, a graph of the propagation length according to the amount of debris flow was plotted. The amount of debris flow was set from 4,000 m^3 to 8,000 m^3. Then, a graph of the propagation length according to entrainment was drawn and compared with the graph on the amount of debris flow. Growth rate is an indicator of entrainment, and was set from 0.01 m^{-1} to 0.03 m^{-1}.

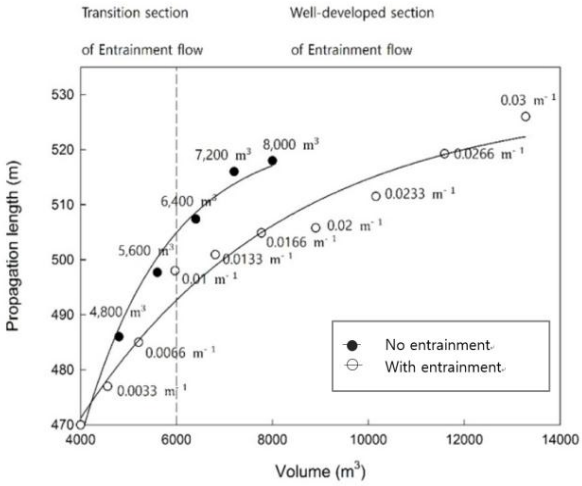

Figure 6: Comparison of the propagation lengths of the debris flow according to the initial amount of debris flow and growth rate. Volume is the total amount of debris flow.

The propagation length and the initial amount of debris flow were calculated using an exponential form similar to previous studies. The rate of increase of the propagation length gradually decreased with the increase of the amount of debris flow, and the tendency of exponential form could be confirmed by an existing study [23]. This means that if the amount of debris flow is predicted, the propagation length can be calculated approximately. The graph including entrainment showed patterns different from the other graph that did not include entrainment in Figure 6. To analyze these patterns, we studied the effect of a change in the growth rate. The characteristic of entrainment was not displayed clearly with $\bar{E} < 0.01$ m^{-1}. Like this phenomenon, the graph ($\bar{E} < 0.01$ m^{-1}) shows a similar pattern to the graph based on changing the amount of debris flow. However, when $\bar{E} > 0.01$ m^{-1}, the propagation length increased slightly even if the amount of debris flow increased. This is a distinct difference from the graph where entrainment was not taken into account. Based on this analysis, we suggest that there is a tendency for the behavior of the debris flow to change around $\bar{E} > 0.01$ m^{-1} or when the total amount of debris flow is 1.5 times the initial amount of debris flow. Through these changed features, we can assume that the transition section and the well-developed section by entrainment. This critical behavior of the debris flow is approximately explained by the debris flow mechanism of entrainment.

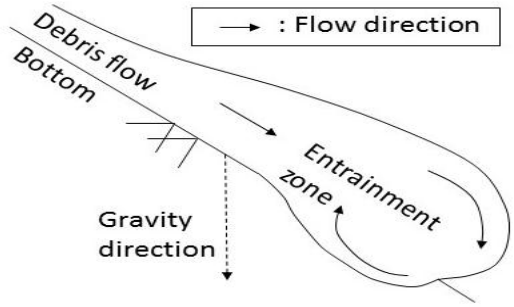

Figure 7: Concept of entrainment in the debris flow

Figure 7 shows that the flow direction changed in rotationally downward to the gravity flow at the front of the debris flow. Therefore, entrainment can interfere with the gravity dominated flow of the debris flow. This suggests that the propagation length can be reduced due to interference from the entrainment or the momentum force. We examined what conditions led to a change in the momentum force related entrainment. According to Figure 8, this occurs when the total amount of debris flow is approximately 1.5 times the initial amount of debris flow. If the point at which the amount of debris flow is 1.5 times can be predicted, it can identify the point where the momentum force is changed by entrainment. The propagation length of debris flow can be calculated easily if the growth rate related to entrainment and the initial amount of debris flow are known. In USGS experimental results, there is a results of verifying the paragraph point above. Comparing the experimental results in Figure 2, we can confirm that the propagation length with consideration of entrainment is 3-5 m less than case of not considering entrainment.This proves the assumption of this study that the propagation length can be reduced due to interference from the entrainment or the momentum force.

6. Results and Discussion

In additional analysis, we changed the values of the growth rate and the entrainment length, which are an index representing the entrainment. These conditions showed how the behavior of the debris flow changed due to changes in the entrainment. The entrainment length was also changed because it is related with the total amount of debris flow. The growth rate and the entrainment length were set at values that were around 1.5 times the total amount of debris flow and the initial amount of debris flow. Through result of Figure 8, the changes in the behavior of the debris flow due to entrainment began in the section above the set value. The growth rates ranged from 0.003 m^{-1} to 0.018 m^{-1}. The entrainment length was varied from 5 m to 40 m.

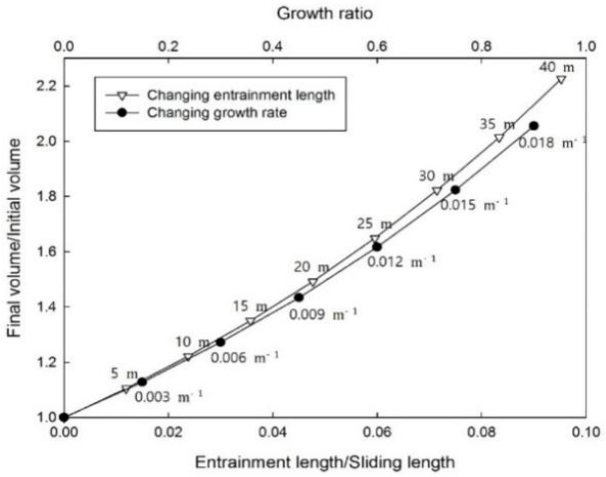

Figure 8: Difference between the final and initial volumes based on growth rate and entrainment length

Figure 9 shows numerical results about the relationship between Froude number and ratio of final volume to initial volume of debris flows when the averaged growth ratio was 0.02 m^{-1}, the entrainment length was 420 m, the final volume was the total amount of debris flow, and the initial volume was the original amount of debris flow. When the growth rate and entrainment length were changed with a constant rate, no singularities were found. The change of entrainment indicates that none of the gravity dominated flow of the debris flow changed into entrainment flow. No singularity was found and the influence of entrainment could not be analyzed in the above method. To solve this analytical issue, we needed a method to directly observe the gravity dominated flow and selected a non-dimensional analysis method of debris flow.

Table 5: Dimensionless parameters related with debris flow propagation

Name	Runout	Bagnold number	Friction number	Mass number	Particle Reynolds number	Savage number	Froude Number
Parameter	L/H	$\frac{\phi\rho_s d^2 u}{(1-\phi)\mu\square}$	$\frac{\phi(\rho_s-\rho_t)d^2\square^2}{(1-\phi)\mu u}$	$\frac{\phi \quad \rho_s}{(1-\phi)\,\rho_f}$	$\frac{\rho_f u d}{\mu}$	$\frac{\rho_s d^2 u^2}{(\rho_s-\rho_t)g\square^3}$	$\frac{u}{\sqrt{gh\cos\theta}}$

The order of magnitude estimates of related dimensionless parameters are listed up in Table 5 where ϕ the solid volume fraction, the solid sand and fluid densities respectively, d the particle diameter, u the flow depth and velocity at front, g the acceleration due to gravity, and θ the slope angle [2].The Froude number in Table 5 is only included to consider gravity dominated flow. The Froude number is the number determined by the depth of the flow, and the gravity and velocity of the flow. Typically, it varies between 0.6 and 10 in a debris flow. A large Froude number indicates a sudden debris flow. In this simulation, the Froude number ranged from 3 to 4.5; and did not change much depending on the initial amount of debris flow. However, the Froude number changed based on entrainment. The analysis was conducted to compare the maximum Froude number of the debris flow with and without inclusion of entrainment. The results show a turning point that is similar to Figure 6. This point represents the change of behavior of the debris flow with entrainment, where the ratio of the initial amount of debris flow to the total amount of debris flow was 1.5 times. Therefore, this method can show the characteristics of the debris flow behavior caused by entrainment or gravity dominated flow.

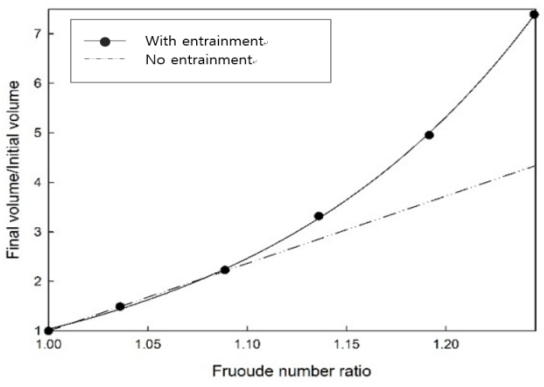

(a)

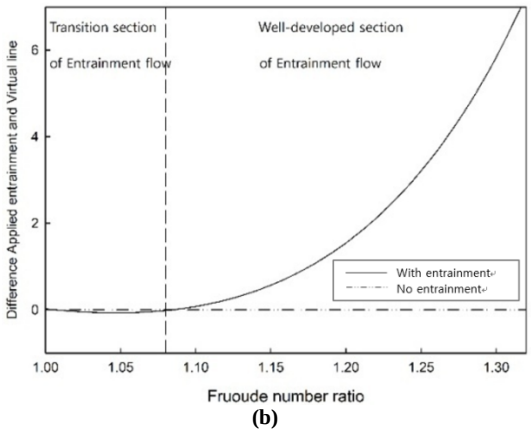

(b)

Figure 9: Relationship between the Froude Number and the volume of debris flow by growth rate related entrainment.

The Froude number ratio is compared with the maximum Froude number of the debris flow when entrainment is not considered, and the maximum Froude number of the debris flow when entrainment is considered in Figure 9(a). We defined that the maximum Froude number of the flow without entrainment is 3.6, the final volume is the total amount of debris flow, and the initial volume is the original amount of debris flow. The criteria that do not influence entrainment are indicated by the dashed line. Difference between two graph values in Figure 9(b) was obviously found, which was confirmed that the final amount of debris flow and the initial amount of debris flow differed 1.5 times at a Froude number ratio of 1.03. This point shows the characteristics of the entrainment, which were found in Figure 8. When the growth rate is greater than 0.013 m^{-1}, the influence of entrainment is significantly increased. The Froude number increased abruptly when comparing the ratio of the increasing entrainment. This result implies that the Froude number can be used to calculate the entrainment phenomenon, which existing studies can hardly predict the behavior of debris flow because they don't count on it. If the Froude number is predicted to be greater than 1.03, the propagation length of the debris flow will be less than the length with no entrainment due to the change of the momentum force or gravity dominated flow. Also, Figure 9(b) shows that we can discern the well-developed section of entrainment flow by checking the Froude number greater than 1.08. This trend was already confirmed in Figure 6. Therefore, when entrainment is predicted approximately, it is possible to estimate a change in the amount of the debris flow in the terrain so that the behavior of the debris flow can be more accurately calculated according to the change in momentum force. This result can complement topographical analyses of the behavior of a debris flow.

7. Conclusion

This study was based on the change of propagation length according to the conditions of a debris flow. The propagation length is often predicted according to the form of an exponent graph, and is predicted using topography and the amount of debris flow. However, this type of analysis cannot consider the change in the momentum force, which is one of the main characteristics of a debris flow. The change in the momentum force of a debris flow is caused by entrainment. Therefore, when entrainment is considered, the propagation length should be calculated in a different form from not considering entrainment. We also found that the behavior of a debris flow is dominated by entrainment. The Froude number was used to analyze the characteristic of entrainment. Figure 10 representing the Froude number clearly shows the change of behavior of the debris flow with entrainment. These results express the behavior of a debris flow that is caused by a change in momentum force represented by Figure 6. This tendency indicates that entrainment is influenced by the momentum force, and the propagation length of a debris flow becomes less than that when not considering entrainment. In addition, these results can be used to improve the limitations of previous analysis methods of the behavior of a debris flow in existing studies that only consider the topography and amount of debris flow. When designing and planning disaster mitigation facilities for debris flows, the overall design may be overestimated if the propagation length is calculated only with the predicted amount of debris flow. By considering entrainment phenomenon, the overestimate can be corrected to appropriate one. This method can also reduce the uncertainty of existing researches and will be useful in debris flow researches where uncertainty becomes high. The results from this study can provide debris flow studies with optimization results.

Acknowledgments

This work was supported by the National Research Foundation of Korea (NRF) grant funded by the Korea government (MSIT) (NRF-2017R1A2B2011990

References

[1] Jakob, M., Hungr, O., &Jakob, D. M. (2005). ***Debris-flow hazards and related phenomena*** (Vol. 739). Berlin: Springer.

[2] Turnbull, B., Bowman, E. T., & McElwaine, J. N. (2015). Debris flows: experiments and modelling. ***ComptesRendus Physique,****16*(1), 86-96.

[3] Hungr, O., Morgan, G. C., & Kellerhals, R. (1984). Quantitative analysis of debris torrent hazards for design of remedial measures. ***Canadian Geotechnical Journal***, *21*(4), 663-677.

[4] Takahashi, T., & Nakagawa, H. (1991). Prediction of stony debris flow induced by severe rainfall. ***Journal of the Japan Society of Erosion Control Engineering***, *44*(3), 12-19.

[5] Takahashi, T. (2014). ***Debris flow: mechanics, prediction and countermeasures***. CRC press.

[6] Schürch, P., Densmore, A. L., Rosser, N. J., Lim, M., &McArdell, B. W. (2011). Detection of surface change in complex topography using terrestrial laser scanning: application to the Illgraben debris- flow channel. ***Earth Surface Processes and Landforms***, *36*(14), 1847-1859.

[7] Gregoretti, C., Adams, M. S., Hagen, K., Laigle, D., Liebault, F., Degetto, M., & Tiranti, D. (2012). Forecast System Guidelines Debris Flows. Guidelines for the Implementation of Forecast System Against Debris Flow Hazard (WP6), Ver 1. 24.12. 2012, Project PARAmountimProved Accessibility: Reliability and Security of Alpine Transport Infrastructure Related to Mountainous Hazards in a Changing Climate, Alp. Space. ***Eur. Reg. Dev. Fund, Brussels***.

[8] Papa, M., Egashira, S., & Itoh, T. (2004). Critical conditions of bed sediment entrainment due to debris flow. ***Natural Hazards and Earth System Sciences***, *4*(3), 469-474.

[9] Cao, Z., Pender, G., Wallis, S., & Carling, P. (2004). Computational dam-break hydraulics over erodible sediment bed. ***Journal of hydraulic engineering***, *130*(7), 689-703.

[10] Pirulli, M., & Pastor, M. (2012). Numerical study on the entrainment of bed material into rapid landslides. ***Geotechnique***, *62*(11), 959.

[11] McCoy, S. W., Kean, J. W., Coe, J. A., Tucker, G. E., Staley, D. M., & Wasklewicz, T. A. (2012). Sediment entrainment by debris flows: In situ measurements from the headwaters of a steep catchment. ***Journal of Geophysical Research: Earth Surface***, *117*(F3).

[12] Song, C. G., & Lee, S. O. (2014). Hydraulic Characteristics of Dam Break Flow by Flow Resistance Stresses and Initial Depths. ***Journal of Korea Water Resources Association***, *47*(11), 1077-1086.

[13] O'Brien, J. S. (2007). FLO-2D user manual. Nutrioso, Arizona

[14] Hungr, O., McDougall, S., & Bovis, M. (2005). Entrainment of material by debris flows. In ***Debris-flow hazards and related phenomena*** (pp. 135-158). Springer, Berlin, Heidelberg..

[15] Song, C. G., Ku, T. G., Kim, Y. D., & Park, Y. S. (2017). Floodplain Stability Indices for Sustainable Waterfront

Development by Spatial Identification of Erosion and Deposition. ***Sustainability***, *9*(5), 735.

[16] McDougall, S., & Hungr, O. (2005). Dynamic modelling of entrainment in rapid landslides. ***Canadian Geotechnical Journal***, *42*(5), 1437-1448.

[17] Iverson, R. M., Logan, M., LaHusen, R. G., & Berti, M. (2010). The perfect debris flow? Aggregated results from 28 large- scale experiments. ***Journal of Geophysical Research: Earth Surface***, *115*(F3).

[18] Reid, M. E., Iverson, R. M., Logan, M, LaHusen, R. G., Godt, J. W., & Griswold, J. P. (2011). Entrainment of bed sediment by debris flows: results from large-scale experiments. In ***Fifth International Conference on Debris-flow Hazards Mitigation, Mechanics, Prediction and Assessment,*** pp. 367-374.

[19] Iverson, R. M. (2012). Elementary theory of bed- sediment entrainment by debris flows and avalanches. ***Journal of Geophysical Research: Earth Surface***, *117*(F3).

[20] Iverson, R. M., Reid, M. E., Logan, M., LaHusen, R. G., Godt, J. W., & Griswold, J. P. (2011). Positive feedback and momentum growth during debris-flow entrainment of wet bed sediment**.** ***Nature Geoscience***, *4*(2), 116.

[21] Mcdougall, S. (2006). A new continuum dynamic model for the analysis of extremely rapid landslide motion across complex 3D terrain. (PhD Thesis). University of British Columbia, Vancouver, USA.

[22] Lee, J. S. (2016) *Behavior of debris flow about entrainment using numerical model*. (Master Thesis). Hongik University, Seoul, Korea.

[23] Lee, J. S.; Song, C. G.; Lee, S. O. (2015), Analysis of Characteristic of Debris Flow with Angle of Slope, *Journal of the Korean Society of Safety*, 31(2), 49-56.